Hindawi Publishing Corporation
Journal of Spectroscopy
Volume 2016, Article ID 5868170, 11 pages
http://dx.doi.org/10.1155/2016/5868170

Research Article

Detection of Melamine in Soybean Meal Using Near-Infrared Microscopy Imaging with Pure Component Spectra as the Evaluation Criteria

Zengling Yang,[1] Lujia Han,[1] Chengte Wang,[1] Jing Li,[1,2] Juan A. Fernández Pierna,[3] Pierre Dardenne,[3] and Vincent Baeten[3]

[1]*College of Engineering, China Agricultural University, Haidian District, Beijing 100083, China*
[2]*Engineering College, Jiangxi Agricultural University, Nanchang 330045, China*
[3]*Valorisation of Agricultural Products Department, Walloon Agricultural Research Centre (CRA-W), Henseval Building, 24 Chaussée de Namur, 5030 Gembloux, Belgium*

Correspondence should be addressed to Lujia Han; hanlj@cau.edu.cn

Received 27 July 2016; Accepted 30 August 2016

Academic Editor: Antonio A. Dos Santos

Soybean meal was adulterated with melamine with the purpose of boosting the protein content for unlawful interests. In recent years, the near-infrared (NIR) spectroscopy technique has been widely used for guaranteeing food and feed security for its fast, nondestructive, and pollution-free characteristics. However, there are problems with using near-infrared (NIR) spectroscopy for detecting samples with low contaminant concentration because of instrument noise and sampling issues. In addition, methods based on NIR are indirect and depend on calibration models. NIR microscopy imaging offers the opportunity to investigate the chemical species present in food and feed at the microscale level (the minimum spot size is a few micrometers), thus avoiding the problem of the spectral features of contaminants being diluted by scanning. The aim of this work was to investigate the feasibility of using NIR microscopy imaging to identify melamine particles in soybean meal using only the pure component spectrum. The results presented indicate that using the classical least squares (CLS) algorithm with the nonnegative least squares (NNLS) algorithm, without needing first to develop a calibration model, could identify soybean meal that is both uncontaminated and contaminated with melamine particles at as low a level as 50 mg kg^{-1}.

1. Introduction

Soybean meal is one of the most important feed raw materials and one of the main ingredients in compound feed because it has a complete protein profile. In the past decade, the price of soybean meal has tripled (http://faostat3.fao.org/home/index.html). The price is dictated by the protein content: the higher the content, the higher the price. There have been recent cases of soybean meal being adulterated with melamine (1,3,5-triazine-2,4,6-triamine) in order to boost the protein content [1]. There have also been cases where it was suspected that soybean meal had been contaminated with low melamine levels. The reference methods (wet chemistry) usually are time-consuming and expensive, cause damage to the sample, and need chemical reagent [2–5]. So there is a real need for fast, nondestructive, and automatically controlled screening methods that will guarantee quality and security.

Near-infrared (NIR) spectroscopy is widely used in this context because it is a rapid, nondestructive, and nonpolluting method that requires minimum or no sample preparation [6]. Applications vary from sample chemical composition to detecting adulteration or contaminant ingredients in raw materials and compound feed [7, 8]. Many studies have investigated the feasibility of using NIR to detect melamine [9–14], but there are still some problems here when it comes to testing samples with low melamine content because of the instrument noise and sampling design error [15, 16]. NIR can

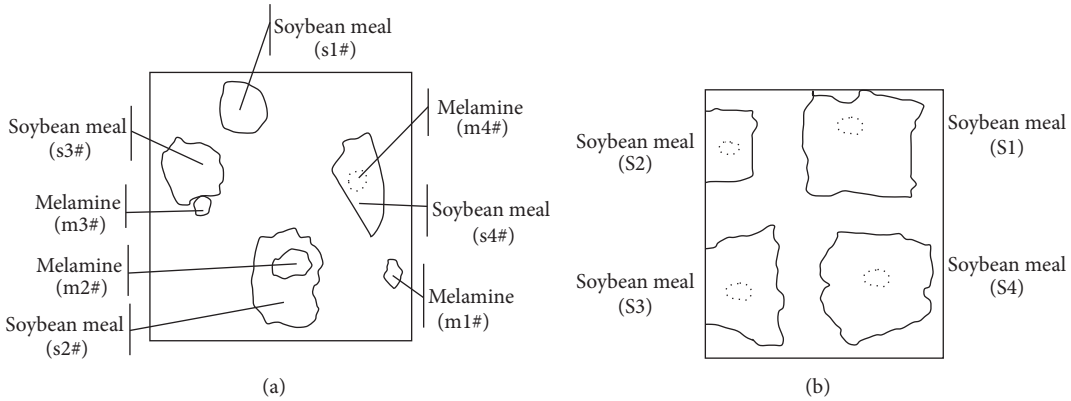

Figure 1: Experimental sample: (a) Set A-1; (b) Set A-2, melamine: line of dashes.

only acquire the spectra information but cannot provide the spatial information of the sample. NIR microscopy (NIRM) which combines NIR and digital images together is able to collect the spectrum of individual particles (the minimum spot size is a few micrometers) from samples [17]. With the development of a high-precision X-Y motion stage, NIRM imaging is obtained by successively measuring spectra while the sample is repositioned in the X and Y spatial dimensions. Thus, the technique offers an opportunity to explore not only what kinds of chemical species are present at the microscale level, but also where they might be present [18].

NIRM imaging is a type of NIR imaging and has better spatial resolution. In the past decade, NIR imaging has become a powerful analytical tool for detecting contaminants and defects in agrofood products [19–25]. For feed products, several investigations have been conducted on the feasibility of using NIRM to detect, identify, and quantify processed animal byproducts [26–30] and on using NIR imaging for the complete screening of compound feeds [31].

The aim of this study was to investigate the feasibility of using NIRM imaging to identify melamine particles in soybean meal. The classical least squares (CLS) algorithm with the nonnegative least squares (NNLS) algorithm was used for the analysis of soybean meal adulterated with melamine.

2. Materials and Methods

2.1. Experimental Design. A total of 20 soybean meal samples were collected from various feed manufacturers and were ground to pass through a 0.5 mm sieve. And 3 melamine samples were bought from three chemical reagent companies, with 99% of the particles being less than 0.25 mm (analytical reagent, $C_3H_6N_6$ content certified by the company ≥99.5%). For this study, three sets of samples were used. Set A was prepared artificially in order to develop a method without the need to create the calibration model. Set B was prepared using representative matrixes to validate the reliability and robustness of the method. Set C was prepared with low melamine content in order to investigate the sensitivity of the method.

2.1.1. Experimental Sample: Set A. Samples were artificially prepared on Teflon Spectralon using soybean meal and melamine particles (Set A-1, Figure 1(a)): a melamine particle (m2#) was placed on top of a soybean meal particle (s2#); a melamine particle (m4#) was placed under a soybean meal particle (s4#); a melamine particle (m3#) and a soybean meal particle (s3#) were clustered together; a single melamine particle (m1#) was used alone; and a single soybean meal particle (s1#) was used alone.

If a melamine particle is placed under a soybean meal particle, the thickness of the latter would affect the detection of the melamine particle. In order to study how this thickness affected the method, other samples were artificially prepared with different soybean meal thicknesses (Set A-2, Figure 1(b)). S1, S2, S3, and S4 relate to soybean meal that was about 30, 50, 100, and 110 μm thick, respectively.

2.1.2. Experimental Sample: Set B. For Set B, using 20 soybean meal and 3 melamine samples, 20 sample mixtures contaminated with 5, 10, 25, and 50 g kg^{-1} of melamine, respectively, with five replicate samples for each melamine content level, were prepared with a mixer (REAX 20/8; Heidolph, Schwabach, Germany) in the laboratory (Table 1). In order to achieve a homogeneous distribution of melamine in the soybean meal, a stepwise dilution procedure was applied to ensure that in each dilution step the ratio of the two materials to be mixed did not exceed a factor of 3 [32].

2.1.3. Experimental Sample: Set C. As shown in Table 1, 4 sample mixtures contaminated with 1,000, 500, 100, and 50 mg kg^{-1} of melamine, respectively, were prepared in the laboratory using 4 soybean meal and 3 melamine samples.

2.2. Data Acquisition. All the samples (Set A, Set B, Set C, and 20 pure soybean meal and 3 pure melamine samples) were analyzed using a NIRM imaging system (Spotlight400, Perkin Elmer), with 16 spectra being acquired simultaneously from the line detector. The detector in this instrument is a mercury cadmium telluride (HgCdTe or MCT). The spatial resolution of scanning is 25 × 25 μm and the spectral resolution is

Table 1: Description of the samples Set B and Set C.

Soybean meal sample number	Melamine sample number	Set B		Set C	
		Sample number	Melamine (g kg^{-1})	Sample number	Melamine (mg kg^{-1})
Soy 1	Mel 1	Set B1	5	Set C1	1,000
Soy 2	Mel 2	Set B2	5	Set C2	500
Soy 3	Mel 3	Set B3	5	Set C3	100
Soy 4	Mel 1	Set B4	5	Set C4	50
Soy 5	Mel 2	Set B5	5	/	/
Soy 6	Mel 3	Set B6	10	/	/
Soy 7	Mel 1	Set B7	10	/	/
Soy 8	Mel 2	Set B8	10	/	/
Soy 9	Mel 3	Set B9	10	/	/
Soy 10	Mel 1	Set B10	10	/	/
Soy 11	Mel 2	Set B11	25	/	/
Soy 12	Mel 3	Set B12	25	/	/
Soy 13	Mel 1	Set B13	25	/	/
Soy 14	Mel 2	Set B14	25	/	/
Soy 15	Mel 3	Set B15	25	/	/
Soy 16	Mel 1	Set B16	50	/	/
Soy 17	Mel 2	Set B17	50	/	/
Soy 18	Mel 3	Set B18	50	/	/
Soy 19	Mel 1	Set B19	50	/	/
Soy 20	Mel 2	Set B20	50	/	/

32 cm^{-1}. Ratio spectra ($R = R_{\text{sample}}/R_{\text{teflon}}$) were collected using a Teflon Spectralon (Spectralon® Targets, Labsphere, Inc., North Sutton, New Hampshire) as the reflectance standard and then converted into absorbance (A) by $A = \log_{10}(1/R)$. Each spectrum was the average of four scans across the wavenumber range of 7,808–4,000 cm^{-1}.

One image (an area of 8.75 × 8.75 mm coupled with 350 × 350 pixels; 122,500 spectra) was scanned for each of Set B and Set C (samples with 1,000, 500, and 100 mg kg^{-1} melamine), respectively. In Set C, four images of samples with 50 mg kg^{-1} melamine were scanned, because it was more difficult to identify melamine particles at low concentrations.

One image (an area of 1.25 × 1.25 mm coupled with 50 × 50 pixels; 2,500 spectra) was scanned for each of the 20 pure soybean meal and 3 pure melamine samples.

2.3. Data Analysis

2.3.1. Preprocessing. The main purpose of preprocessing was to remove spectral and spatial artifacts such as rough surfaces, optic effects, and detector noise. The NIRM imaging data cube and the pure component spectra were both preprocessed by applying a first derivative using the Savitzky-Golay algorithm with a five-point filter width and a degree 2 polynomial [33]. The noisy part at the end of the spectra was removed by reducing the spectral range to between 7,300 and 4,100 cm^{-1}.

2.3.2. Chemometric Tools. The classical least squares (CLS) algorithm was used to extract melamine distribution maps from whole wavelengths [34, 35]. This algorithm is a suitable method involving minimizing the sum of squared residuals in order to predict concentrations using reference spectra only. It was based on the assumption that the absorbance spectra from a pixel in NIRM imaging can be viewed as the weighted sum of the absorbance of each pure component spectrum constituting the sample, as well as the experimental noise. Initially, the data cube ($x \times y \times \lambda$) was unfolded into a two-dimensional matrix $X = (xy \times \lambda)$. Matrix X was then decomposed as follows:

$$X = CS^T + E, \tag{1}$$

where S^T represents the pure component signals; C is the relative concentration matrix; and E is the error matrix.

C was estimated by the pseudoinverse $C = XS(S^tS)^{-1}$ using the nonnegative least squares (NNLS) algorithm. The concentration of melamine and soybean meal, respectively, was then calculated as follows [36]:

$$C_{\text{mel}} = 1000 \times \frac{\sum_{i=1}^{n} C_i}{\left(\sum_{i=1}^{n} C_i + \sum_{j=1}^{n} C_j\right)},$$
$$C_{\text{soy}} = 1000 \times \frac{\sum_{j=1}^{n} C_j}{\left(\sum_{i=1}^{n} C_i + \sum_{j=1}^{n} C_j\right)}, \tag{2}$$

where C_{mel} (g kg^{-1}) is the melamine concentration of sample; C_i is the melamine concentration of each pixel in the NIRM image predicted by CLS; C_j is the soybean meal concentration of each pixel in the NIRM image predicted by CLS; n is the number of pixels in one NIRM image; and C_{soy} (g kg^{-1}) is the soybean meal concentration of the sample.

All C_i or C_j values formed a chemical image in which higher pixel intensity reflected higher target concentration. Matlab® (The MathWorks, http://www.mathworks.com/) and the PLS Toolbox (Eigenvector Research, http://www.eigenvector.com/) were used to perform this analysis.

3. Results and Discussion

3.1. Soybean Meal and Melamine Component Spectra. The melamine reference spectrum was obtained by averaging all the pixel spectra of 3 pure melamine images, and the soybean meal reference spectrum was obtained by averaging all the pixel spectra of 20 pure soybean meal images (Figure 2). Melamine is a triazine heterocyclic organic compound, composed of nitrogen heterocyclic rings and -NH_2. The NIR region offers a special advantage in the measurement of the primary amine NH_2 group because of a unique combination band [37]. Melamine has three strong characteristic peaks in the 6,900–6,450 cm^{-1} range, especially near 6,805 cm^{-1}, which is the N-H combination band (νN-H asymmetric and νN-H symmetric combination) from primary amides. Figure 2 showed that melamine has a distinctive spectral feature compared with soybean meal, facilitating the identification of melamine particles present in mixtures.

3.2. Soybean Meal Analysis Using CLS. Table 2 showed the minimum C_j of 20 soybean meal samples which were calculated by CLS. Meanwhile, the mean value of the minimum values of C_j is 0.8822 and the standard deviation is 0.0484. In consideration of the conciseness and effectiveness, the liminal value of soybean meal's C_j was 0.8.

3.3. Melamine Detection Using CLS. Figure 3 showed the detection results of Set A samples using CLS algorithm. Figure 3(a) was a soybean meal image produced by CLS. Four soybean meal particles (s1#, s2#, s3#, and s4#) could be correctly identified. Figure 3(b) showed a melamine image produced by CLS. CLS could detect the presence of melamine m1#, m2#, and m3#, but not m4# which was placed under a 150 μm thick soybean meal particle. In order to investigate the effect of soybean meal thickness on the detection of melamine under the soybean meal particle using the CLS algorithm, an image of sample Set A-2 was obtained and analyzed using CLS. When the soybean meal was 30 μm and 50 μm thick, CLS could detect the presence of melamine, but it could not do so if the melamine was under soybean meal that was thicker than 100 μm. In addition, the signal of the melamine under soybean meal that was 50 μm thick was weaker than the signal when the thickness was 30 μm, illustrating the difficulty of detecting the presence of melamine when melamine particles were embedded in soybean meal particles.

Table 2: The minimum C_j of 20 soybean meal samples calculated by CLS.

Sample number	Min of C_j
Soy 1	0.9387
Soy 2	0.8099
Soy 3	0.9317
Soy 4	0.9358
Soy 5	0.9278
Soy 6	0.7671
Soy 7	0.8276
Soy 8	0.9322
Soy 9	0.9008
Soy 10	0.8214
Soy 11	0.8721
Soy 12	0.9315
Soy 13	0.9084
Soy 14	0.8611
Soy 15	0.8941
Soy 16	0.8941
Soy 17	0.9036
Soy 18	0.8479
Soy 19	0.8702
Soy 20	0.8677

Sample Set B containing 20 contaminated samples were analyzed using the CLS algorithm and the results were shown in Table 3. The concentrations of melamine calculated by CLS were 0.84±0.30, 3.51±0.75, 8.17±1.21, and 32.23±4.33 g kg^{-1} for the 5, 10, 25, and 50 g kg^{-1} melamine content samples, respectively. The melamine in the 20 mixture samples was successfully detected. Although the melamine concentration was underestimated by CLS, there was a good linear relationship between the predicted and real values (predicted values = 0.57 × real values, R^2 = 0.90). Particle size, surface roughness, and density of the sample spread on a Teflon Spectralon surface in a single layer were important factors in quantifying melamine correctly. It is also likely that the melamine concentration was underestimated because of the difficulty in detecting melamine if the particles were under or tightly embedded in the soybean meal particles, as shown in sample Set A.

The pixel spectra corresponding to the C_i maximum of melamine for the 20 sample mixtures are shown in Figure 4. These melamine spectral characteristics indicated reliable extraction by CLS. In addition, the results showed that NIRM imaging data combined with the CLS algorithm could provide a visual melamine distribution map (Figure 5) for the analyst, which could not be done by NIR because the spatial information is lost.

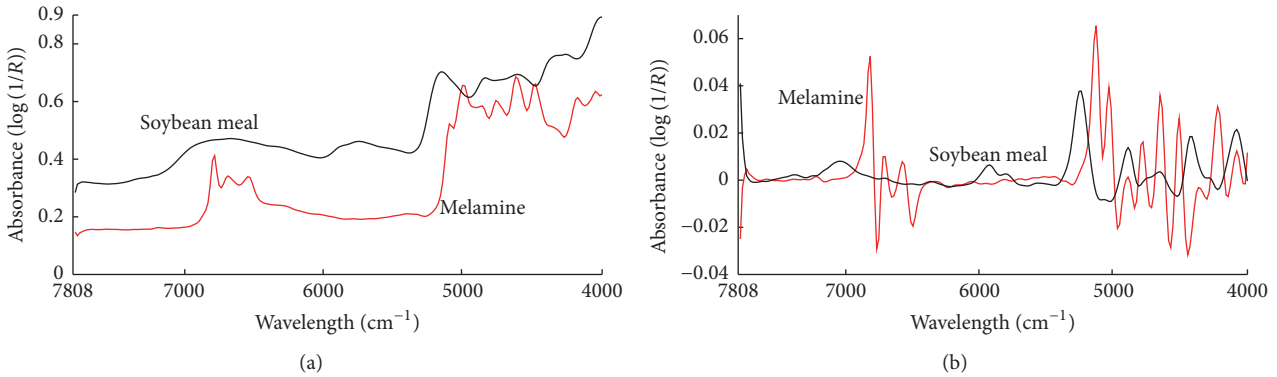

Figure 2: Average spectrum of soybean meal and melamine particles: raw spectra (a) and first derivative spectra (b).

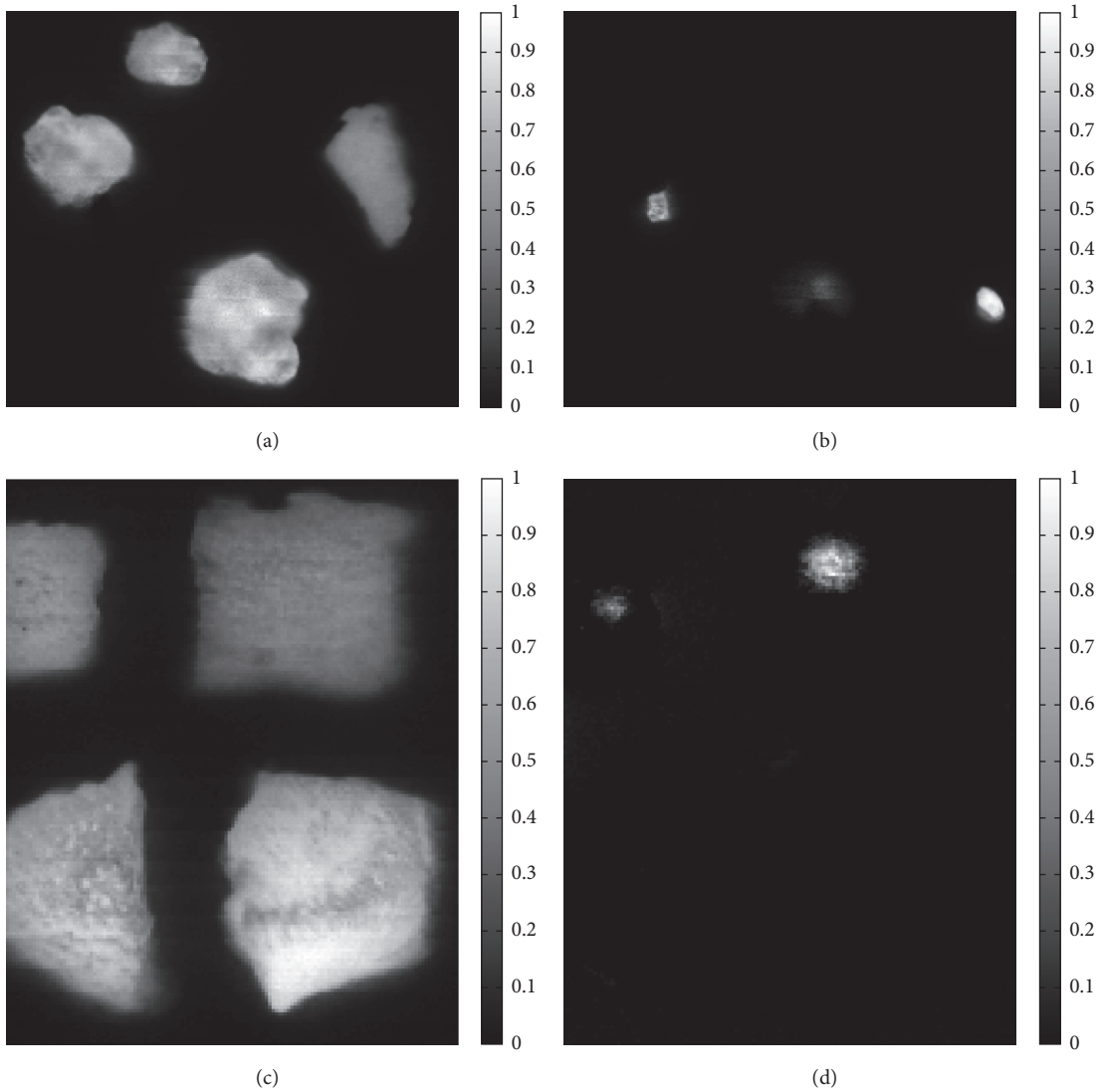

Figure 3: The detection results of soybean and melamine of Set A samples using CLS algorithm: (a) soybean image of Set A-1; (b) melamine image of Set A-1; (c) soybean image of Set A-2; (d) melamine image of Set A-2.

Table 3: Discriminant results of the analysis of the Set B samples using CLS.

Sample number	Melamine ($g\,kg^{-1}$)	Melamine detected		
		C_{mel} ($g\,kg^{-1}$)	Max of C_i	Number of spectra
Set B1	5	1.16	1.0919	1,955
Set B2	5	1.01	0.7524	1,897
Set B3	5	0.92	0.6206	1,959
Set B4	5	0.41	0.5971	1,337
Set B5	5	0.67	0.5686	1,509
Set B6	10	3.06	0.6696	6,635
Set B7	10	3.27	0.8080	6,449
Set B8	10	3.53	0.8891	7,865
Set B9	10	2.91	0.7721	7,998
Set B10	10	4.78	0.9064	10,871
Set B11	25	8.54	0.9536	21,913
Set B12	25	7.03	0.5367	25,188
Set B13	25	6.74	0.7325	15,940
Set B14	25	9.18	0.8827	19,452
Set B15	25	9.35	0.7916	39,533
Set B16	50	37.22	0.9413	90,127
Set B17	50	28.71	0.8753	81,584
Set B18	50	34.09	0.5128	106,041
Set B19	50	26.78	0.6352	89,335
Set B20	50	34.37	0.6912	101,457

Sample Set C was used to investigate the method's sensitivity. $C_j < 0.8$ and GH > 3 were combined together for melamine detection in sample Set C. The GH is the standardized Mahalanobis distance between each spectrum and average spectrum, and GH > 3 is used to identify the outliers [38, 39]. In this work, 480 representative spectra were picked out from the 20 pure soybean meal images. And the GH values between the target spectrum and the 480 soybean spectra were calculated to identify whether the target spectrum is soybean spectrum or not.

As shown in Figure 6, all the 1000, 500, and 100 $mg\,kg^{-1}$ of melamine images had spectra out of both GH and C_j liminal values. Two of four 50 $mg\,kg^{-1}$ melamine images had spectra out of both GH and C_j liminal values. Using GH and C_j liminal values to analyze 20 pure soybean meal samples, there were also some abnormal spectra in Soy 6. The abnormal spectra detected by $C_j < 0.8$ and GH > 3 of Set C and Soy 6 were shown in Figure 7. All the spectra separated from Set C had the melamine spectra characteristics which could be recognized by visual inspection. Meanwhile the spectra separated from Soy 6 were not similar with melamine spectrum or soybean meal average spectrum; this part of the spectra was more like full-fat soybean which could be seen in the article published by Shen et al. [39].

4. Conclusions

The results presented in this study showed the feasibility of the NIRM imaging with pure component spectra for the analysis of soybean meal adulterated with melamine. The minimum effective detection concentration of melamine was 50 $mg\,kg^{-1}$. NIRM imaging method is a nondestructive, pollution-free, and cheaper testing technology compared with wet chemical analysis method, and it could analyze one sample within four hours. NIRM imaging combined with the CLS algorithm can successfully detect melamine in soybean meal without building the calibration model, which provided a new and feasible way for safety control of feed.

Competing Interests

The authors declare that there is no conflict of interests regarding the publication of this paper.

Acknowledgments

The research leading to these results was funded by the European Union's Seventh Framework Program (FP7/2007–2013) under Grant Agreement 265702 (Quality and Safety

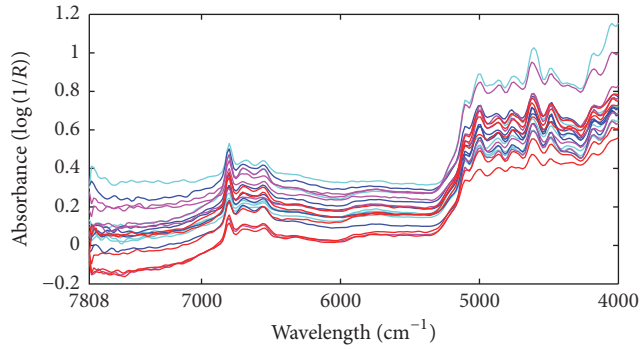

FIGURE 4: The pixel spectra corresponding to the C_i maximum of melamine for Set B samples: 5 g kg^{-1} (cyan), 10 g kg^{-1} (blue), 25 g kg^{-1} (magenta), and 50 g kg^{-1} (red).

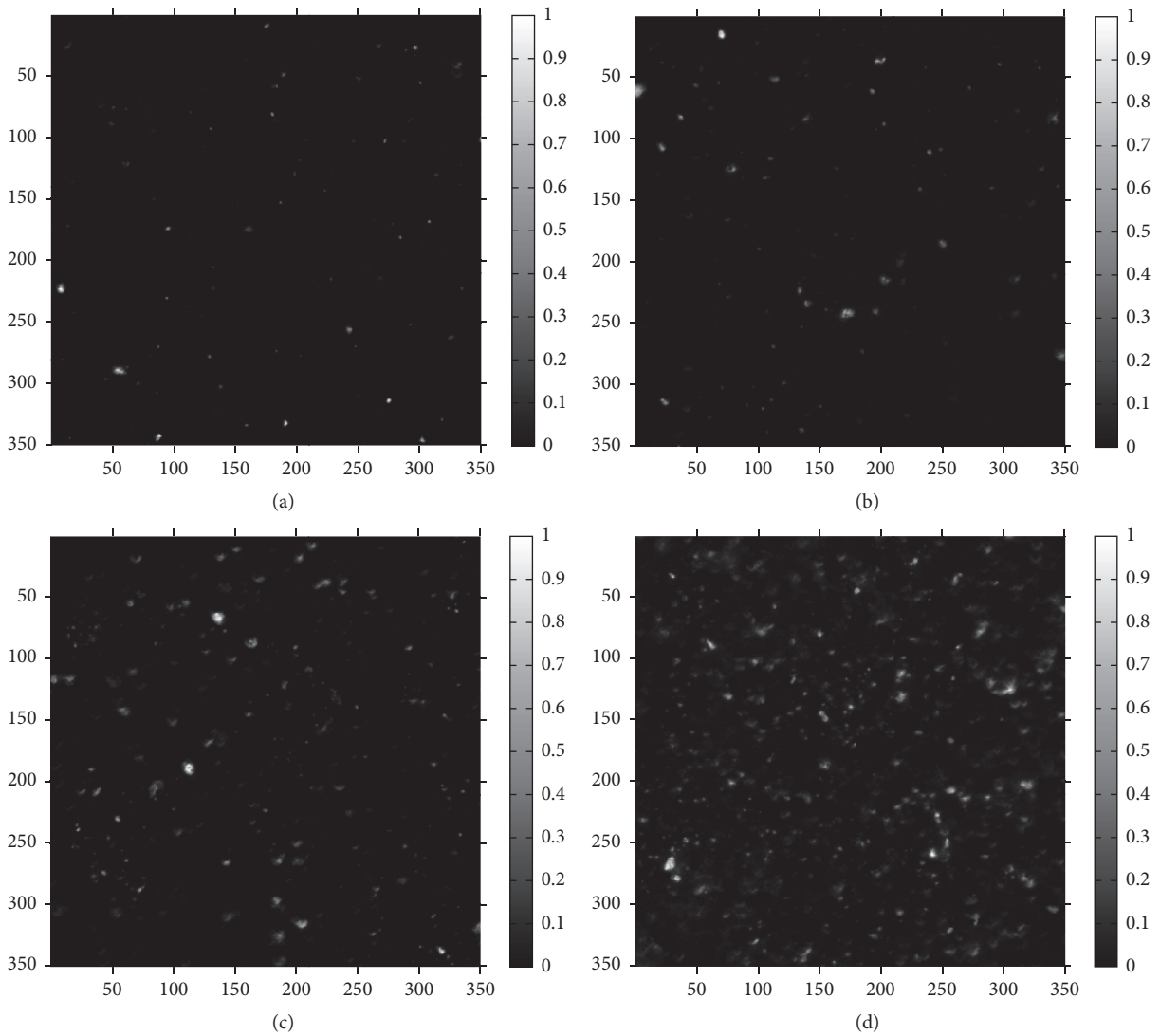

FIGURE 5: The melamine distribution map predicted by CLS applied to the NIRM imaging data. Only one sample was taken as an example of each concentration. (a), (b), (c), and (d) represent 5, 10, 25, and 50 g kg^{-1} of melamine, respectively.

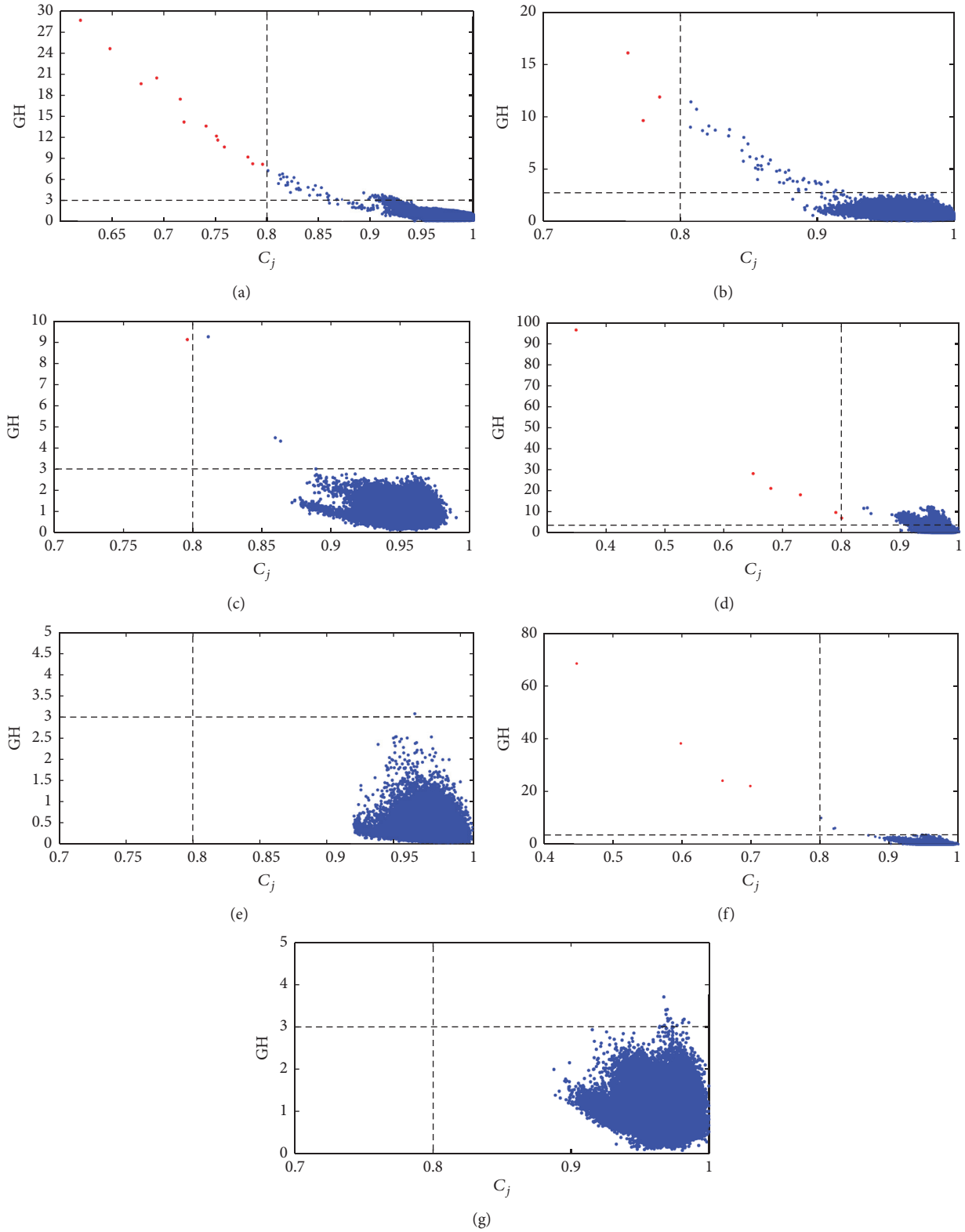

FIGURE 6: The C_j-GH diagram of Set C. (a), (b), and (c) represent 1000, 500, and 100 mg kg^{-1} of melamine images, while (d), (e), (f), and (g) represent four 50 mg kg^{-1} of melamine images.

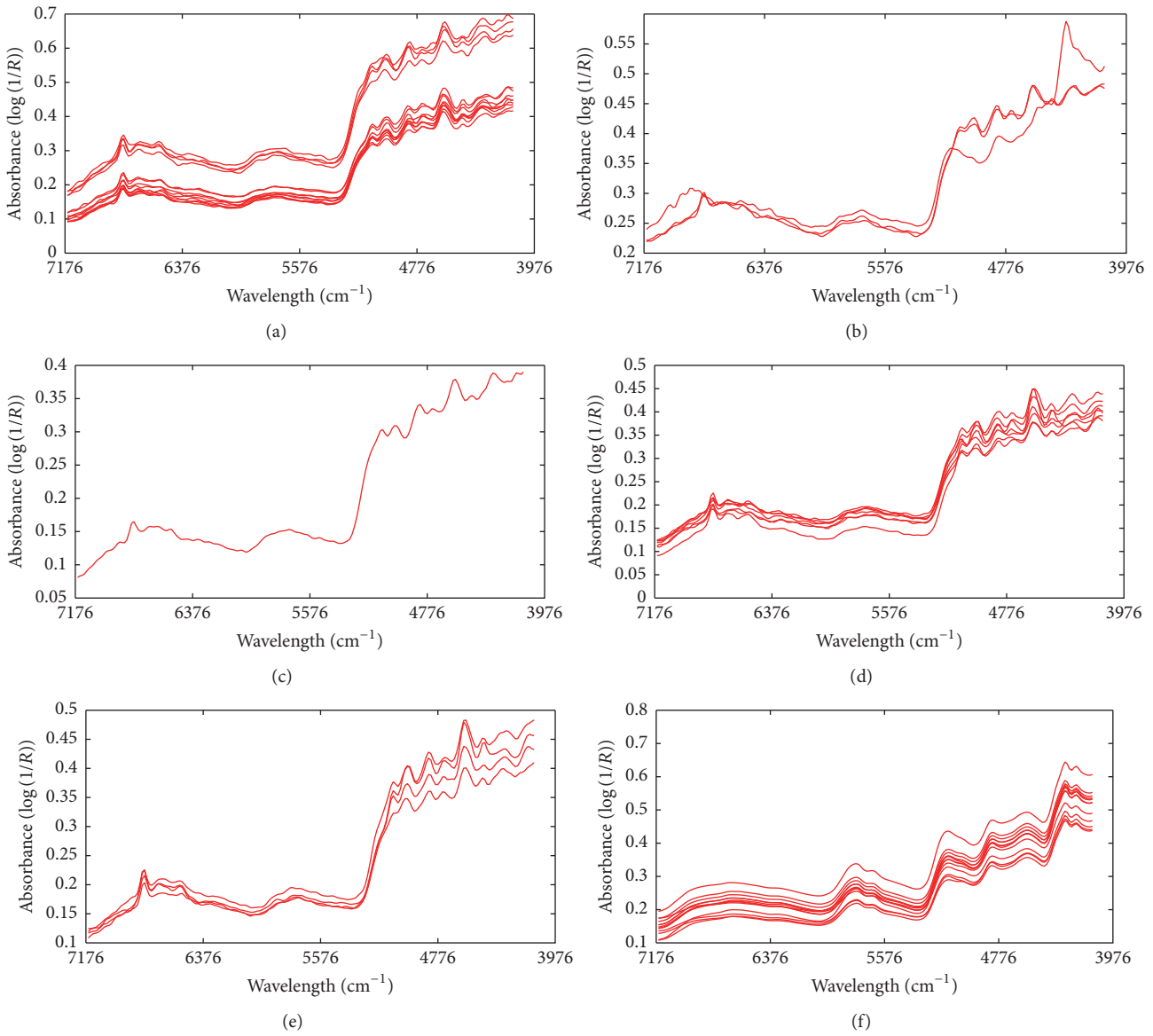

FIGURE 7: The spectra out of both GH and C_j liminal values. (a), (b), and (c) represent 1000, 500, and 100 mg kg^{-1} of melamine images, (d) and (e) represent two 50 mg kg^{-1} of melamine images, and (f) represents Soy 6 image.

of Feeds and Food for Europe, QSAFFE), National Science and Technology Support Program (2014BAD08B11-2), Program of International S&T Cooperation (Project no. 2015DFG32170), and the Bruxelles-Wallonie International Cooperation Project between the Walloon Agricultural Research Centre (CRA-W) in Gembloux, Belgium, and the China Agricultural University (CAU) in Beijing, China. The authors would also like to thank Jiang Xunpeng and Chen Qianrong for their help in data processing and experimental design.

References

[1] J. L. Dorne, D. R. Doerge, M. Vandenbroeck et al., "Recent advances in the risk assessment of melamine and cyanuric acid in animal feed," *Toxicology and Applied Pharmacology*, vol. 270, no. 3, pp. 218–229, 2013.

[2] G. Venkatasami and J. R. Sowa, "A rapid, acetonitrile-free, HPLC method for determination of melamine in infant formula," *Analytica Chimica Acta*, vol. 665, no. 2, pp. 227–230, 2010.

[3] L. Zhao, J. Zhao, W.-G. Huangfu, and Y.-L. Wu, "Simultaneous determination of melamine and clenbuterol in animal feeds by GC-MS," *Chromatographia*, vol. 72, no. 3-4, pp. 365–368, 2010.

[4] S. Squadrone, G. L. Ferro, D. Marchis et al., "Determination of melamine in feed: validation of a gas chromatography-mass spectrometry method according to 2004/882/CE regulation," *Food Control*, vol. 21, no. 5, pp. 714–718, 2010.

[5] S. Turnipseed, C. Casey, C. Nochetto et al., "Determination of melamine and cyanuric acid residues in infant formula using LC-MS/MS ," *Laboratory Information Bulletin*, vol. 4421, pp. 496–549, 2008.

[6] L. Chen, Z. Yang, and L. Han, "A review on the use of near-infrared spectroscopy for analyzing feed protein materials," *Applied Spectroscopy Reviews*, vol. 48, no. 7, pp. 509–522, 2013.

[7] V. Baeten, M. Manley, and J. A. Fernández Pierna, "Spectroscopic techniques: Fourier Transform (FT) Near Infrared spectroscopy (NIR) and microscopy (NIRM)," in *Modern Techniques for Food Authentication*, D.-W. Sun, Ed., pp. 117–148, Academic Press, Oxford, UK, 2008.

[8] J. A. Fernández Pierna, V. Baeten, and A. Boix, "Detection, identification and quantification of processed animal proteins in feedingstuffs," in *Near Infrared Microscopy*, J. S. Jorgensen and V. Baeten, Eds., pp. 81–91, Les Presses Universitaires de Namur, Namur, Belgium, 2012.

[9] C. Lu, B. Xiang, G. Hao, J. Xu, Z. Wang, and C. Chen, "Rapid detection of melamine in milk powder by near infrared spectroscopy," *Journal of Near Infrared Spectroscopy*, vol. 17, no. 2, pp. 59–67, 2009.

[10] L. J. Mauer, A. A. Chernyshova, A. Hiatt, A. Deering, and R. Davis, "Melamine detection in infant formula powder using near- and mid-infrared spectroscopy," *Journal of Agricultural and Food Chemistry*, vol. 57, no. 10, pp. 3974–3980, 2009.

[11] R. M. Balabin and S. V. Smirnov, "Melamine detection by mid- and near-infrared (MIR/NIR) spectroscopy: a quick and sensitive method for dairy products analysis including liquid milk, infant formula, and milk powder," *Talanta*, vol. 85, no. 1, pp. 562–568, 2011.

[12] S. A. Haughey, S. F. Graham, E. Cancouët, and C. T. Elliott, "The application of Near-Infrared Reflectance Spectroscopy (NIRS) to detect melamine adulteration of soya bean meal," *Food Chemistry*, vol. 136, no. 3-4, pp. 1557–1561, 2013.

[13] S. Jawaid, F. N. Talpur, S. T. H. Sherazi, S. M. Nizamani, and A. A. Khaskheli, "Rapid detection of melamine adulteration in dairy milk by SB-ATR-Fourier transform infrared spectroscopy," *Food Chemistry*, vol. 141, no. 3, pp. 3066–3071, 2013.

[14] O. Abbas, B. Lecler, P. Dardenne, and V. Baeten, "Detection of melamine and cyanuric acid in feed ingredients by near infrared spectroscopy and chemometrics," *Journal of Near Infrared Spectroscopy*, vol. 21, no. 3, pp. 183–194, 2013.

[15] K. Norris, "Hazards with near infrared spectroscopy in detecting contamination," *Journal of Near Infrared Spectroscopy*, vol. 17, no. 4, pp. 165–166, 2009.

[16] V. Baeten and P. Dardenne, "Applications of near-infrared imaging for monitoring agricultural food and feed products," in *Spectrochemical Analysis Using Infrared Multichannel Detectors*, R. Bhargava and I. W. Levin, Eds., pp. 283–302, Blackwell, 2005.

[17] Z. Yang, C. Wang, L. Han, J. Li, and X. Liu, "Rapid screening and visual tracing of melamine in soybean meal by NIR microscopy imaging," *Journal of Innovative Optical Health Sciences*, vol. 7, no. 4, Article ID 1350072, 2014.

[18] F. Clarke, "Extracting process-related information from pharmaceutical dosage forms using near infrared microscopy," *Vibrational Spectroscopy*, vol. 34, no. 1, pp. 25–35, 2004.

[19] J. Dubois, E. Neil Lewis, F. S. Fry Jr., and E. M. Calvey, "Bacterial identification by near-infrared chemical imaging of food-specific cards," *Food Microbiology*, vol. 22, no. 6, pp. 577–583, 2005.

[20] D. P. Ariana, R. Lu, and D. E. Guyer, "Near-infrared hyperspectral reflectance imaging for detection of bruises on pickling cucumbers," *Computers and Electronics in Agriculture*, vol. 53, no. 1, pp. 60–70, 2006.

[21] P. Williams, P. Geladi, G. Fox, and M. Manley, "Maize kernel hardness classification by near infrared (NIR) hyperspectral imaging and multivariate data analysis," *Analytica Chimica Acta*, vol. 653, no. 2, pp. 121–130, 2009.

[22] J. P. Wold, M. O'Farrell, M. Høy, and J. Tschudi, "On-line determination and control of fat content in batches of beef trimmings by NIR imaging spectroscopy," *Meat Science*, vol. 89, no. 3, pp. 317–324, 2011.

[23] R. Krska and M. Nielen, "Rapid detection in food and feed," *Analytical and Bioanalytical Chemistry*, vol. 405, no. 24, pp. 7717–7718, 2013.

[24] P. Vermeulen, J. A. Fernández Pierna, H. P. van Egmond, P. Dardenne, and V. Baeten, "Online detection and quantification of ergot bodies in cereals using near infrared hyperspectral imaging," *Food Additives & Contaminants: Part A*, vol. 29, no. 2, pp. 232–240, 2012.

[25] Y. Huang, S. Min, J. Duan, L. Wu, and Q. Li, "Identification of additive components in powdered milk by NIR imaging methods," *Food Chemistry*, vol. 145, pp. 278–283, 2014.

[26] V. Baeten, C. Von Holst, A. Garrido, J. Vancutsem, A. M. Renier, and P. Dardenne, "Detection of banned meat and bone meal in feedstuffs by near-infrared microscopic analysis of the dense sediment fraction," *Analytical and Bioanalytical Chemistry*, vol. 382, no. 1, pp. 149–157, 2005.

[27] B. De la Roza-Delgado, A. Soldado, A. Martínez-Fernández et al., "Application of near-infrared microscopy (NIRM) for the detection of meat and bone meals in animal feeds: a tool for food and feed safety," *Food Chemistry*, vol. 105, no. 3, pp. 1164–1170, 2007.

[28] V. Fernández-Ibáñez, T. Fearn, A. Soldado, and B. de la Roza-Delgado, "Spectral library validation to identify ingredients of compound feedingstuffs by near infrared reflectance microscopy," *Talanta*, vol. 80, no. 1, pp. 54–60, 2009.

[29] D. Pérez-Marín, T. Fearn, J. E. Guerrero, and A. Garrido-Varo, "A methodology based on NIR-microscopy for the detection of animal protein by-products," *Talanta*, vol. 80, no. 1, pp. 48–53, 2009.

[30] O. Abbas, J. A. Fernández Pierna, A. Boix, C. Von Holst, P. Dardenne, and V. Baeten, "Key parameters for the development of a NIR microscopic method for the quantification of processed by-products of animal origin in compound feedingstuffs," *Analytical and Bioanalytical Chemistry*, vol. 397, no. 5, pp. 1965–1973, 2010.

[31] J. A. Fernández Pierna, V. Baeten, and P. Dardenne, "Screening of compound feeds using NIR hyperspectral data," *Chemometrics and Intelligent Laboratory Systems*, vol. 84, no. 1-2, pp. 114–118, 2006.

[32] G. Gizzi, C. von Holst, V. Baeten, G. Berben, and L. Van Raamsdonk, "Determination of processed animal proteins, including meat and bone meal, in animal feed," *Journal of AOAC International*, vol. 87, no. 6, pp. 1334–1341, 2004.

[33] C. Gendrin, Y. Roggo, and C. Collet, "Pharmaceutical applications of vibrational chemical imaging and chemometrics: a review," *Journal of Pharmaceutical and Biomedical Analysis*, vol. 48, no. 3, pp. 533–553, 2008.

[34] K. L. A. Chan, N. Elkhider, and S. G. Kazarian, "Spectroscopic imaging of compacted pharmaceutical tablets," *Chemical Engineering Research and Design*, vol. 83, no. 11, pp. 1303–1310, 2005.

[35] G. P. Sabin, M. C. Breitkreitz, A. M. de Souza et al., "Analysis of pharmaceutical pellets: an approach using near-infrared chemical imaging," *Analytica Chimica Acta*, vol. 706, no. 1, pp. 113–119, 2011.

[36] C. Gendrin, Y. Roggo, and C. Collet, "Content uniformity of pharmaceutical solid dosage forms by near infrared hyperspectral imaging: a feasibility study," *Talanta*, vol. 73, no. 4, pp. 733–741, 2007.

[37] L. Weyer and J. Workman Jr, *Practical Guide to Interpretive Near-Infrared Spectroscopy*, CRC Press, 2007.

[38] J. A. Guthrie, *Robustness of NIR Calibrations for Assessing Fruit Quality*, Faculty of Arts, Health and Sciences, Central Queensland University, 2005.

[39] G. Shen, X. Fan, Z. Yang, and L. Han, "A feasibility study of non-targeted adulterant screening based on NIRM spectral library of soybean meal to guarantee quality: the example of non-protein nitrogen," *Food Chemistry*, vol. 210, pp. 35–42, 2016.